NANO LETTERS

2007
Vol. 7, No. 5
1338−1343

Plasmonic Nanosensors for Imaging Intracellular Biomarkers in Live Cells

Sonia Kumar,[†] Nathan Harrison,[†] Rebecca Richards-Kortum,[‡] and Konstantin Sokolov*[,†,§]

Department of Biomedical Engineering, University of Texas at Austin, Austin, Texas 78712, Department of Bioengineering, Rice University, Houston, Texas 77005, and Department of Biomedical Engineering, University of Texas M.D. Anderson Cancer Center, Houston, Texas 77030

Received February 14, 2007; Revised Manuscript Received March 30, 2007

ABSTRACT

Here we present the first intracellular molecular imaging platform using multifunctional gold nanoparticles which incorporate both cytosolic delivery and targeting moieties on the same particle. The utility of these intracellular sensors was demonstrated by monitoring actin rearrangement in live fibroblasts. We observed a strong molecular specific optical signal associated with effective targeting of actin filaments. These multifunctional nanosensors can be adapted to target various intracellular processes especially where transfection or cytotoxic labels are not feasible.

As the age of molecular medicine progresses, it has become increasingly vital that we fully understand the molecular pathways and progenitors of disease. Both quantum dots and plasmonic nanoparticles have shown great promise in visualizing these pathways.[1−10] Gold nanoparticles have recently been exploited for the direct monitoring of molecular interactions in DNA hybridization kinetics and the arrangement of receptors on the surface of cancerous cells.[8,10] Optical signal is based on the fact that metal nanoparticles resonantly scatter light upon excitation of the surface plasmon.[11] Properties such as photostability, water solubility, and nontoxicity make these probes highly advantageous for biological imaging. Optical contrast between isolated and closely spaced gold nanoparticles can be achieved by exploiting changes in intensity and peak wavelength based on the distance-dependent scattering properties of the nanoparticles.[5,9,12,13] While a solution of isolated 20 nm gold nanoparticles scatter light at approximately 520 nm, closely spaced assemblies can shift that resonance on the order of 100 nm giving a brighter red signal.[13] Inducing the close proximity of plasmonic particles in the presence of a specific target can therefore provide a sensor to probe molecular interactions.[10,12,13] The assembly formation by nanoparticles can be mediated by targeting molecules such as antibodies that interact with the biomarker of interest.

Probes to visualize molecular features have two basic requirements: accessing the target and providing a meaningful signal.[4,14] As many interesting biomolecules are located inside the cell, access to the target must involve a delivery mechanism. Here we report multifunctional plasmonic nanoparticles for intracellular imaging in living cells which incorporate both cytosolic delivery and targeting moieties on the same particle. We showed that these sensors can be effectively delivered into the cytoplasm and can bind to their target providing strong molecular specific optical signal. The utility of this contrast agent was demonstrated in the intracellular imaging of actin during cellular motility. Actin was chosen as a target because of its importance in enhancing cell−biomaterial interactions as well in its deregulation during disease.[15,16] The vast abundance of actin, often micromolar concentrations, makes it necessary to discriminate filaments involved in active polymerization from a sea of actin monomers.[17−19] Plasmonic nanoparticles are ideal for investigating such filaments since they provide contrast enhancement in closely spaced assemblies.

Monodisperse, water-soluble 20 nm gold nanoparticles were synthesized via citrate reduction of chloroauric acid (HAuCl4) as described by Frens et al.[20] Then, anti-actin and anti-biotin antibodies were attached to gold nanoparticles via a heterofunctional linker that consists of an alkane terminating in a dithiol tether and an amide-bonded adipic hydrazide (Sensopath, SPT-0014b). Monoclonal anti-actin antibodies were specific for the C-terminal end which is conserved in both G- and F-actin isoforms. Monoclonal anti-biotin antibodies were used for the attachment of biotinylated TAT-HA2 peptide. Briefly, glycosylated antibodies (1 mg/mL) in 100 mM $NaHPO_4$ (pH ∼7.5) were reacted in the dark with 100 mM $NaIO_4$ in a 1:10 volume ratio for 30 min to oxidize

* Corresponding author. E-mail: kostia@mail.utexas.edu. Phone: 512 471 7440. FAX: 512 471 0616.
† University of Texas at Austin.
‡ Rice University.
§ University of Texas M.D. Anderson Cancer Center.

10.1021/nl070365i CCC: $37.00
Published on Web 04/17/2007

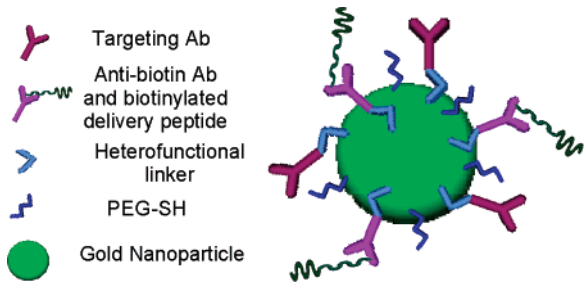

Figure 1. Multifunctional contrast agent. Schematic representation of gold nanoparticle based contrast agent with both targeting and delivery components.

the carbohydrate on the Fc portion of the antibody to an aldeyhde.[21] The presence of aldehydes was verified using PurPald reagent (Sigma) in 1 N NaOH. The reaction was then quenched with 1xPBS and an excess of the heterofunctional linker was added to the oxidized antibody. The solution was incubated for at least 1 h to allow the hydrazide (linker) and aldeyhde (antibody) to spontaneously react to form a hydrazone bond. By incorporation of a linker on the Fc portion of the antibody, the active Fab portions are directed outward from the contrast agent and are therefore available for targeting.[21,22] The linker-bound antibody was then purified using a Centricon 10kMWCO filter (Millipore) and resuspended in 40 mM HEPES, pH 8.5, to a working concentration of 0.067 mg/mL. For conjugation to gold nanoparticles, 1 mL of 20 nm gold nanoparticle solution (10^{12} particles/mL) was added to a premixed solution of 50 μL of linker-bound anti-actin antibody and 50 μL of linker-bound anti-biotin antibody. The solution was incubated for 20 min. Then, 100 μL of 10^{-5} M 5000 MW PEG-SH (Shearwater) was added to coat the remaining exposed gold surfaces. The hydrophilic nature of PEG also improves the biocompatibility of the conjugate. Finally, biotinyated TAT-HA2 (Biotin-Cys-Lys-Tyr-Gly-Arg-Arg-Arg-Gln-Arg-Arg-Lys-Lys-Arg-Gly-Gly-Asp-Ile-Met-Gly-Glu-Trp-Gly-Asn-Glu-Ile-Phe-Gly-Ala-Ile-Ala-Gly-Phe-Leu-Gly-OH) was added to react with the anti-biotin antibodies for 20 min. The gold bioconjugates were centrifuged at 4000*g* for 30 min in the presence of 100 μL of 2% 15000 MW PEG (Sigma) to prevent aggregation. A schematic representation of the contrast agent is shown in Figure 1. These nanoparticles incorporate four functionalities on a single entity: targeting, endosomal uptake, endosomal release, and improved biocompatibility through PEG. The cytosolic delivery of these molecular nanosensors was mediated by TAT-HA2 peptides. TAT protein transduction domain was recently shown to be taken up by the cell in a receptor-independent form of endocytosis known as lipid raft-mediated macropinocytosis.[23] However, the endosomal membrane must be disrupted to achieve the cytosolic delivery. The pH-sensitive influenza virus hemagglutinin protein HA2 disrupts the integrity of the endosomal lipid membrane at low pH releasing the endosomal content into the cytosol without being cytotoxic like other endosomal membrane destabilizers such as polyethylenimine.[23] The TAT-HA2 sequence is therefore a fusogenic transduction peptide that can be used to enhance both the endocytic uptake and the subsequent endosomal release of an imaging contrast agent. The attachment of TAT-HA2 has been proven effective in the cytosolic delivery of superparamagnetic nanoparticles.[24]

The contrast agents were validated in live NIH3T3 fibroblasts using both darkfield reflectance (DR) with white light illumination and transmission electron microscopy (TEM). NIH3T3 fibroblasts were grown in a humidified incubator at 37 °C, 5% CO_2 and maintained in completed DMEM (with 5% fetal bovine serum and 5% glutamine/penicillin/streptomycin). Cells were deposited on coverslips partially coated with collagen IV and allowed to settle for 4 h prior to labeling. A 1 mL solution of approximately 10^{11} nanoparticles/mL in completed phenol-free DMEM was applied to each coverslip for 30 min at 37 °C to label the cells. Coverslips were washed with fresh media prior to imaging. Darkfield images with white light xenon illumination were taken using a Leica DM 6000 upright microscope equipped with a 20×, 0.95 NA darkfield objective and a Q-Imaging Retiga EXi ultrasensitive 12-bit CCD camera. The DR image in Figure 2a shows increased signal intensity at the leading edge of the cell as it moves toward a chemoattractant, collagen IV.[25] The yellow-orange color of the leading edge indicates plasmonic coupling between nanoparticles.[5,13] Representative TEM images (parts b and c of Figure 2) verify the source of the optical signal with a high concentration of gold nanoparticles present throughout the extending lamellipodia at the leading edge of the cell. The separation distance between gold nanoparticles, on the order of one diameter or less, validates the strong plasmonic coupling observed in the DR color shift. Since the gold nanoparticle labeling pattern is consistent with traditional post-fixation-labeled TEM images, this may be a valuable tool in streamlining TEM imaging of intracellular events.[26] In order to demonstrate the added functionality of the HA2 peptide in aiding cytosolic delivery, cells were labeled with gold nanoparticles conjugated to anti-actin antibodies and only the TAT portion of the delivery peptide. In these cells, the contrast agent was restricted to endosomal structures throughout the cell as indicated by the arrows in the Figure 2c inlay. Without the endosomal membrane disruption caused by the HA2 peptide, the contrast agent is retained within endosomes and cannot participate in actin labeling.

In order to demonstrate the necessity of each element of the contrast agent, various formulations were created by eliminating one component at a time and tested on NIH3T3 cells. Specific labeling was quantified using a colorimetric assay on the RGB images obtained. Since the plasmonic coupling of gold nanoparticles associated with actin labeling results in a red shift in the reflectance spectra, a ratio of red channel intensity over total intensity was calculated to quantify the degree of labeling. Unlabeled cells (Figure 3a) show the characteristic bluish tinge of native cellular reflectance with only 26% of the signal in the red channel. Cells labeled with gold nanoparticles with anti-actin antibody and only the TAT portion of the delivery peptide show yellow-orange dots that indicate entrapment of the contrast agent in endosomes (Figure 3b). Since the conjugate is not distributed over the cell, cells retain their bluish reflectance and only 20% of the signal is in the red channel. In cells

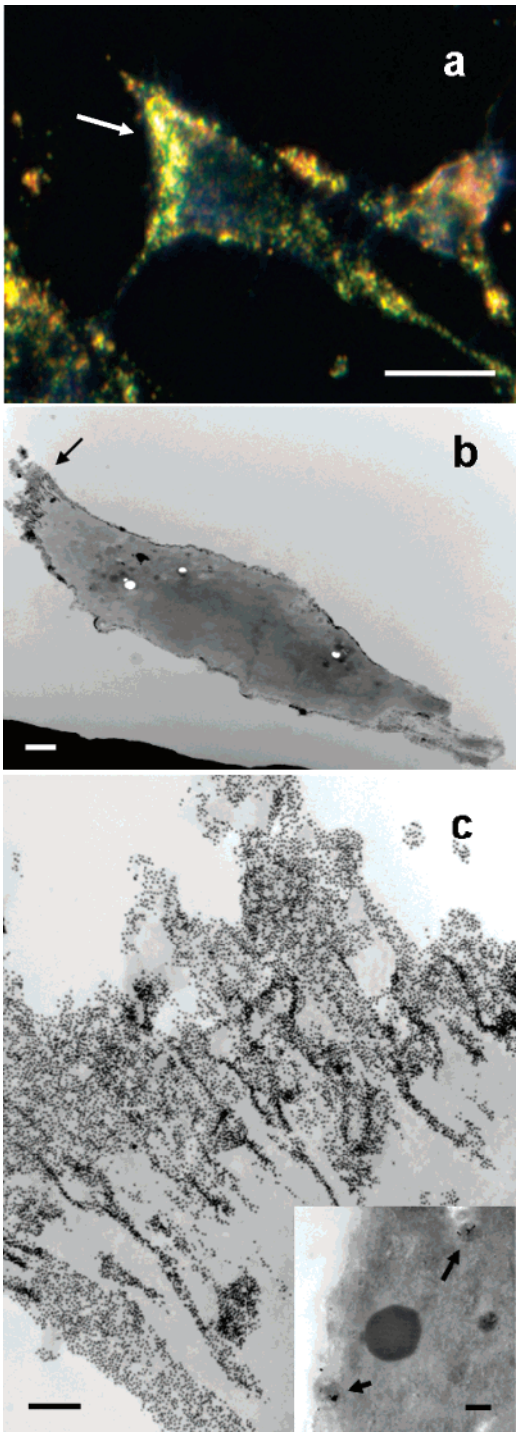

Figure 2. (a) Darkfield reflectance image of a live NIH3T3 cell labeled with gold nanoparticle based contrast agents targeted to actin. The leading edge (arrow) of the cell where actin polymerization is greatest corresponds to a brighter optical signal. Scale bar is 20 μm. (b) TEM image demonstrating delivery of complete multifunctional contrast agent in live NIH3T3 cells. Scale bar is 2 μm. (c) A higher magnification TEM image shows the nanoparticle labeling pattern in the region indicated by the arrow in panel b. The inlay shows live cells labeled with contrast agent containing incomplete delivery peptide (TAT only). Labeling is localized to endosomal structures without HA2 functionality. Scale bars are 0.2 μm.

labeled with gold nanoparticles conjugated to solely anti-actin antibodies (Figure 3c), the image loses the dominance

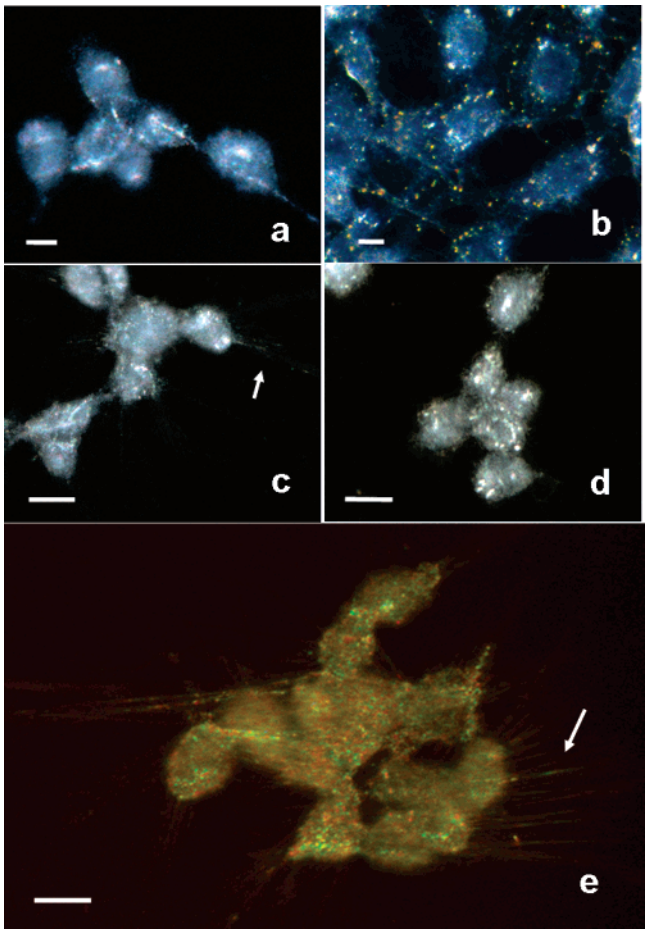

Figure 3. Efficacy of multiple functionalities in labeling intracellular targets. Darkfield reflectance imaging of live NIH3T3 cells labeled with varying 20 nm gold nanoparticle contrast agent formulations: (a) unlabeled cells; (b) contrast agent functionalized with anti-actin targeting antibody and only the TAT delivery peptide; (c) contrast agent functionalized with only anti-actin targeting antibody; (d) contrast agent functionalized with only TAT-HA2 delivery peptide; (e) multifunctional contrast agent with both targeting and delivery moieties. Arrows indicate the presence of visible filapodia. Scale bars are 10 μm.

of blue with a 33% red signal indicating the presence of contrast agent. Lamellipodic extensions also start to become visible. This indicates that a small fraction of contrast agent is taken up by the fibroblasts without the delivery peptide. The contrast agent with only the delivery peptide functionalization also shows increased red signal at 32% (Figure 3d). The absence of lamellipodia indicates that although the contrast agent is entering the cell, which is expected from the activity of delivery peptide, there is no actin-mediated aggregation of the contrast agent and, therefore, there is no appreciable optical contrast. The image of these cells appears to have a punctate pattern. This pattern lacks the distinct yellow-orange color of endosomes containing gold nanoparticles (see Figure 3b) and is likely associated with endogenous scattering from organelles in the cells such as mitochondria. Effective labeling takes advantage of both cytoplasmic delivery and a specific target that decreases the distance between particles thereby resulting in a red shift and an increase in the scattering per particle. Figure 3e shows

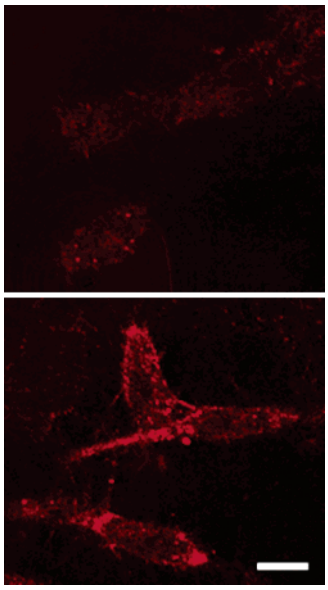

Figure 4. High contrast is achieved in confocal images of NIH3T3 cells labeled with a complete multifunctional contrast agent in labeled cells (bottom) vs unlabeled cells (top). Scale bar is 10 μm.

cells labeled with complete multifunctional contrast agent where the filopodia are easily distinguished and actin fibers are visible. Complete contrast agent increases the signal in the red channel to 52% which is observed as a dramatic color change from predominantly blue in the unlabeled sample to shades of green and orange.

Plasmonic coupling between nanoparticles separated by approximately two diameters or less is primarily responsible for the orange signal.[5] The enhancement of the green is attributed to the coherence scattering of nanoparticles that are separated by distances more than two diameters apart but less than $\lambda/2\pi$, where λ is the wavelength of light.[11,13] The scattering from these nanoparticles increases quadratically with their number without producing a color shift that results in the green shades in labeled cells.[11] Background signal variation between panels in Figure 3 can be attributed to the concentration of contrast agent in the surrounding media**.** Representative brightfield images of fibroblasts are available online in Supporting Information. A similar pattern of labeling was also seen in a Leica SP2 AOBS confocal fluorescence/reflectance microscope using a 633 nm HeNe laser line and 63× water immersion objective (Figure 4). Higher contrast images were obtained in confocal images because detection is limited to 623−643 nm emission which increases sensitivity to closely spaced nanoparticles.

We compared the labeling pattern obtained with complete multifunctional contrast agents in live cells with fluorescent phalloidin staining which is a common F-actin labeling technique in formalin-fixed cells. Confocal fluorescent images of labeled fixed fibroblasts show a distribution of stress fibers throughout the cell (available in Supporting Information online). The labeling pattern seen with plasmonic nanosensors appears to be more sensitive to areas of active actin rearrangement at the leading edge of the cell (Figure 2a). We believe that this pattern is associated with actin mediated assembly of the nanoparticles at the leading edge that results in easily identifiable yellow-orange color in DR images and the quadratic increase in scattering of gold nanoparticles as discussed above. Delivery of the contrast agents through the cellular membrane facilitates labeling of actively forming actin fibers at the leading edge of the cell while fewer nanoparticles diffuse inside the cell.

By use of a modified RC 20 live imaging chamber (Warner Instruments), cells were imaged continuously during and after labeling which enabled the capture of actin dynamics during cellular motility including retraction, extension, and rearrangement. The use of a single-entity contrast agent allowed for a simple visualization of actin with both the uptake of nanoparticles and labeling occurring in less than 5 min. Centripetal shortening of actin fibers was observed approximately 30 min postlabeling during the retraction of lamellipodia as shown in Figure 5 (see video in online Supporting Information). The rate of retraction of the leading edge of the segment of actin filament has an average value of 0.2 μm/s. This result is consistent with previously published values of centripetal retraction in Swiss 3T3 fibroblasts where an average of 0.26 μm/s was observed by attaching and tracking 0.5 μm beads on the dorsal surface of lamellipodia.[27] To monitor actin during cell spreading, cells grown on a monolayer of collagen IV were imaged at various time points. Figure 6 shows time points at 4 and 8 h after cell deposition. At 4 h, actin filaments are arranged in long lamellipodic extensions between cells. At 8 h, actin is aligned at the boundaries between cells as they begin to form a sheet. Actin rearrangement in fibroblasts on a collagen IV substrate and rearrangement at the leading edge of fibroblasts as they crawl toward a collagen IV stimulus are shown online in Supporting Information. Previously, actin monitoring during chemotaxis was carried out using microinjection of fluorescently labeled actin monomers which is both tedious and limiting in the number of cells studied.[28]

We demonstrate here a novel optical contrast agent complete with affinity to an intracellular biomolecule and an efficient cytosolic delivery mechanism. Studying actin in cultured fibroblasts is only one of many biological systems this contrast agent can be adapted for. The conjugation method can easily be extended by incorporating the appropriate antibody to target other intracellular biomarkers of interest such as p16, which is upregulated in cervical cancers.[29] Since TAT-HA2 uses a receptor-independent endocytosis pathway, the contrast agent delivery is not cell specific and should theoretically be effective in other cell types. We have obtained promising preliminary results in labeling the metastatic rat mammary adenocarcinoma cell line MTLn3 (video available in online Supporting Information). We are currently exploring labeling actin filaments to monitor changes in cytoskeletal arrangement in connection with a biological function in live cells. The potential ability of this delivery peptide to penetrate different cell types is particularly useful since a long-term biomarker labeling probe can be invaluable in imaging cells where transfection or cytotoxic labels are not feasible. Gold nanoparticle based sensors can also be used in combination with TEM to provide super high-resolution "snapshots" that can be correlated with

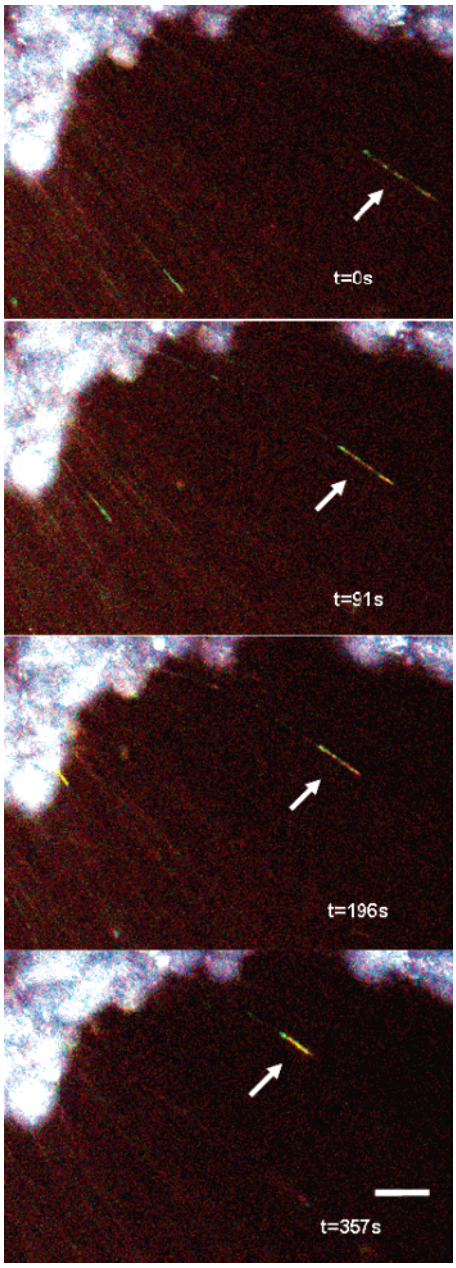

Figure 5. Imaging actin dynamics. Cellular functions involving actin were demonstrated using darkfield reflectance imaging of live NIH3T3 cells labeled with multifunctional contrast agent. Retraction of filapodia is shown here at various time points. Arrows indicate labeled actin filaments. Scale bar is 20 μm.

live optical imaging. The surface conjugation chemistry can also be adapted for additional imaging probes. Quantum dots passivated with a thiol-reactive layer can easily be substituted for gold nanoparticles in this conjugation protocol for applications in which fluorescent signal would be more advantageous.

One potential limitation of gold nanoparticles is the amount that can be loaded in to the cells to achieve a saturation of labeling of targeted biomarkers. The upper concentration is limited by the size of the particle and the density of the labeling solution. To overcome this, the size, shape, and concentration of the nanoparticles would need to be optimized. There is also some uncertainty of the effect of

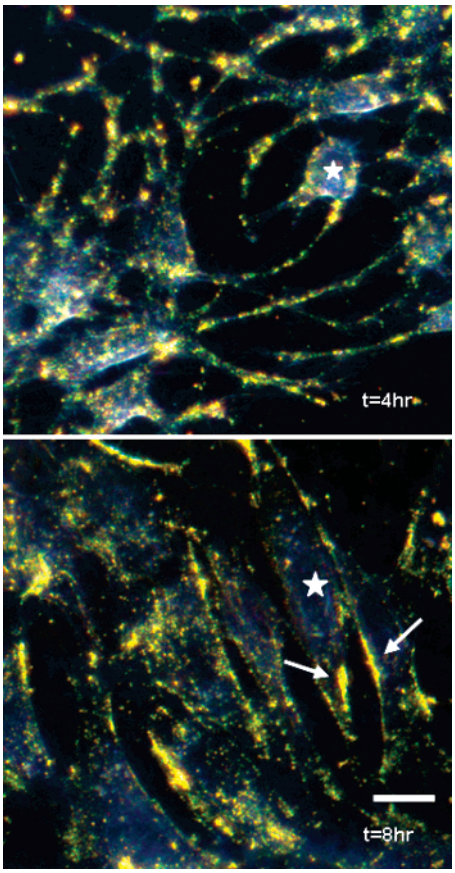

Figure 6. The arrangement of actin is followed as cells spread on a monolayer of collagen IV. Time points at 4 h (top) and 8 h (bottom) are shown. White stars indicate a cell body and arrows indicate actin alignment. Scale bar is 20 μm.

nanoparticles on cellular processes. While there was no indication of any deviant behavior in actin labeling experiments, the presence of nanoparticles may interfere with other molecular interactions. However, our experiments showed that multifunctional gold nanoparticles have great potential as a complementary contrast agent to quantum dots and other probes for the optical imaging of molecular intracellular processes. The plasmon resonance coupling between adjacent nanoparticles provides a unique opportunity to directly image biomolecular interactions like actin rearrangement which is demonstrated in this report.

Acknowledgment. The authors acknowledge Dr. Wolfgang Frey for his helpful comments and discussions. The study was supported by NIH Grant CA103830. S. Kumar was supported by a NSF Integrated Graduate Education and Research Traineeship (IGERT) Grant.

Supporting Information Available: Two images and four videos are available: (image S1) brightfield images of cells with various contrast agent formulations; (image S2) confocal fluorescent image of AlexaFluor488-phallodin stained fixed fibroblasts; (video S1) centripetal shortening during the retraction of lamellipodia; (video S2) actin rearrangement in fibroblasts on a collagen IV substrate; (video S3) the leading edge of fibroblasts as they crawl

toward a collagen IV stimulus; (video S4) MTLn3 adenocarcinoma cells are labeled with multifunctional contrast agent. This material is available free of charge via the Internet at http://pubs.acs.org.

References

(1) Alivisatos, P. The use of nanocrystals in biological detection. *Nat. Biotechnol.* **2004**, *22* (1), 47−52.

(2) Chan, W. C.; Nie, S. Quantum dot bioconjugates for ultrasensitive nonisotopic detection. *Science* **1998**, *281* (5385), 2016−2018.

(3) Liu, G. L.; Yin, Y.; Kunchakarra, S.; Mukherjee, B.; Gerion, D.; Jett, S. D.; Bear, D. G.; Gray, J. W.; Alivisatos, A. P.; Lee, L. P.; Chen, F. F. A nanoplasmonic molecular ruler for measuring nuclease activity and DNA footprinting. *Nat. Nanotechonol.* **2006**, *1* (1), 47−52.

(4) Michalet, X.; Pinaud, F. F.; Bentolila, L. A.; Tsay, J. M.; Doose, S.; Li, J. J.; Sundaresan, G.; Wu, A. M.; Gambhir, S. S.; Weiss, S. Quantum dots for live cells, in vivo imaging, and diagnostics. *Science* **2005**, *307* (5709), 538−544.

(5) Rechberger, W.; et al. Optical properties of two interacting gold nanoparticles. *Opt. Commun.* **2003**, *220*, 137−141.

(6) Reinhard, B. M.; Siu, M.; Agarwal, H.; Alivisatos, A. P.; Liphardt, J. Calibration of dynamic molecular rulers based on plasmon coupling between gold nanoparticles. *Nano Lett.* **2005**, *5* (11), 2246−2252.

(7) Sokolov, K.; Aaron, J.; Hsu, B.; Nida, D.; Gillenwater, A.; Follen, M.; MacAulay, C.; Adler-Storthz, K.; Korgel, B.; Descour, M.; Pasqualini, R.; Arap, W.; Lam, W.; Richards-Kortum, R. Optical systems for in vivo molecular imaging of cancer. *Technol. Cancer Res. Treat.* **2003**, *2* (6), 491−504.

(8) Sokolov, K.; Follen, M.; Aaron, J.; Pavlova, I.; Malpica, A.; Lotan, R.; Richards-Kortum, R. Real-time vital optical imaging of precancer using anti-epidermal growth factor receptor antibodies conjugated to gold nanoparticles. *Cancer Res.* **2003**, *63* (9), 1999−2004.

(9) Sonnichsen, C.; Alivisatos, A. P. Gold nanorods as novel nonbleaching plasmon-based orientation sensors for polarized single-particle microscopy. *Nano Lett.* **2005**, *5* (2), 301−304.

(10) Sonnichsen, C.; Reinhard, B. M.; Liphardt, J.; Alivisatos, A. P. A molecular ruler based on plasmon coupling of single gold and silver nanoparticles. *Nat. Biotechnol.* **2005**, *23* (6), 741−745.

(11) van de Hulst, H. C. *Light Scattering By Small Particles*; Dover: Mineola, 1981.

(12) Aslan, K.; Lakowicz, J. R.; Geddes, C. D. Plasmon light scattering in biology and medicine: new sensing approaches, visions and perspectives. *Curr. Opin. Chem. Biol.* **2005**, *9* (5), 538−544.

(13) Aaron, J.; Nitin, N.; Travis, K.; Kumar, S.; Collier, T.; Park, S. Y.; Jose-Yacaman, M.; Coghlan, L.; Follen, M.; Richards-Kortum, R.; Sokolov, K. Plasmon Resonance Coupling of Metal Nanoparticles for Molecular Imaging of Carcinogenesis In Vivo. *J. Biomed. Opt.*, in press.

(14) Kumar, S.; Richards-Kortum, R. Optical molecular imaging agents for cancer diagnostics and therapeutics. *Nanomedicine* **2006**, *1* (1), 23−30.

(15) Brunton, V. G.; MacPherson, I. R.; Frame, M. C. Cell adhesion receptors, tyrosine kinases and actin modulators: a complex three-way circuitry. *Biochim. Biophys. Acta* **2004**, *1692* (2−3), 121−144.

(16) Owen, G. R.; Meredith, D. O.; ap Gwynn, I.; Richards, R. G. Focal adhesion quantification−a new assay of material biocompatibility? Review. *Eur. Cells Mater.* **2005**, *9*, 85−96; discussion 85−96.

(17) Kuhn, J. R.; Pollard, T. D. Real-time measurements of actin filament polymerization by total internal reflection fluorescence microscopy. *Biophys. J.* **2005**, *88* (2), 1387−1402.

(18) Nicholson-Dykstra, S.; Higgs, H. N.; Harris, E. S. Actin dynamics: growth from dendritic branches. *Curr. Biol.* **2005**, *15* (9), R346−357.

(19) Wang, Y. L. Reorganization of actin filament bundles in living fibroblasts. *J. Cell Biol.* **1984**, *99* (4 Pt 1), 1478−1485.

(20) Frens, G. Controlled Nucleation for the Regulation of the Particle Size in Monodisperse Gold Suspensions. *Nat. Phys. Sci.* **1973**, *241*, 20−22.

(21) Spangler, B. D., Tyler, B. J. Capture agents for a quartz crystal microbalance-continuous flow biosensor: functionalized self-assembled monolayers on gold. *Anal. Chim. Acta* **1999**, *399*, 51−62.

(22) Hermanson, G. T. *Bioconjugate Techniques*; Academic Press: San Diego, 1996.

(23) Wadia, J. S.; Stan, R. V.; Dowdy, S. F. Transducible TAT-HA fusogenic peptide enhances escape of TAT-fusion proteins after lipid raft macropinocytosis. *Nat. Med.* **2004**, *10* (3), 310−315.

(24) Won, J.; Kim, M.; Yi, Y. W.; Kim, Y. H.; Jung, N.; Kim, T. K. A magnetic nanoprobe technology for detecting molecular interactions in live cells. *Science* **2005**, *309* (5731), 121−125.

(25) Hodgson, L.; Qiu, W.; Dong, C.; Henderson, A. J. Use of green fluorescent protein-conjugated beta-actin as a novel molecular marker for in vitro tumor cell chemotaxis assay. *Biotechnol. Prog.* **2000**, *16* (6), 1106−1114.

(26) Willingham, M. C.; Yamada, S. S.; Davies, P. J.; Rutherford, A. V.; Gallo, M. G.; Pastan, I. Intracellular localization of actin in cultured fibroblasts by electron microscopic immunocytochemistry. *J. Histochem. Cytochem.* **1981**, *29* (1), 17−37.

(27) Fisher, G. W.; Conrad, P. A.; DeBiasio, R. L.; Taylor, D. L. Centripetal transport of cytoplasm, actin, and the cell surface in lamellipodia of fibroblasts. *Cell Motil. Cytoskeleton* **1988**, *11* (4), 235−247.

(28) Mallavarapu, A.; Mitchison, T. Regulated actin cytoskeleton assembly at filopodium tips controls their extension and retraction. *J. Cell Biol.* **1999**, *146* (5), 1097−1106.

(29) Klaes, R.; Friedrich, T.; Spitkovsky, D.; Ridder, R.; Rudy, W.; Petry, U.; Dallenbach-Hellweg, G.; Schmidt, D.; von Knebel Doeberitz, M. Overexpression of p16(INK4A) as a specific marker for dysplastic and neoplastic epithelial cells of the cervix uteri. *Int. J. Cancer* **2001**, *92* (2), 276−284.

NL070365I